
Targeting Relative Risk Heterogeneity with Causal Forests

Vik Shirvaikar
University of Oxford

Chris Holmes
University of Oxford

Abstract

Treatment effect heterogeneity (TEH), or variability in treatment effect for different subgroups within a population, is of significant interest in clinical trial analysis. Causal forests (Wager and Athey, 2018) is a highly popular method for this problem, but like many other methods for detecting TEH, its criterion for separating subgroups focuses on differences in absolute risk. This can dilute statistical power by masking nuance in the relative risk, which is often a more appropriate quantity of clinical interest. In this work, we propose and implement a methodology for modifying causal forests to target relative risk using a novel node-splitting procedure based on generalized linear model (GLM) comparison. We present results on simulated and real-world data that suggest relative risk causal forests can capture otherwise unobserved sources of heterogeneity.

1 Introduction

Causal inference methods are frequently employed in clinical studies to analyze the effect of a drug or treatment. In this setting, we are often interested in exploring the evidence for treatment effect heterogeneity (TEH), or whether specific subgroups of the population respond differently to the treatment in question.

An immediate concern with subgroup analysis is the problem of multiple testing (Cook et al., 2004). Analyzing a sufficiently large number of subgroups will inevitably yield spurious false-positive results, and as the dimensionality of a dataset grows, the number of possible ways to divide the population into subgroups increases exponentially. To combat this, most clinical

trial protocols require a subgroup analysis plan to be specified in advance. However, this can prevent the detection of strong but unexpected heterogeneity. TEH discovery therefore calls for nonparametric methods which can consider the dataset as a whole, uncover relevant high-dimensional interactions, and identify subgroups of interest (Watson and Holmes, 2020).

Causal forests, developed by Athey and Imbens (2015) and Wager and Athey (2018), is one of the most successful approaches in this area. It modifies the classical random forests of Breiman (2001), popular for flexible modelling of interactions in high dimensions, to satisfy necessary theoretical criteria for causal inference. Since its introduction, it has become an industry-standard approach for TEH estimation in real-world clinical trial analysis (Basu et al., 2018; Athey and Wager, 2019; Raghavan et al., 2022).

However, the node-splitting criterion in causal forests only targets heterogeneity in the absolute (additive) Risk Difference (RD) between subgroups. This can dilute statistical power for heterogeneity in the relative (multiplicative) Risk Ratio (RR) by over-emphasizing individuals with a high baseline risk level. The resulting TEH estimates may then be targeted towards covariates that are predictive of mortality (or other adverse outcomes) rather than heterogeneity. If there is large variation in individual baseline risk, as seen in the AQUAMAT and LEADER clinical trials we present in Sections 4 and 5, it may be therefore preferable to focus on differences in the RR. The RR also provides benefits related to explanation and generalizability, due to its superior ability to extrapolate across populations (Cook and Sackett, 1995; Colnet et al., 2023).

We therefore aim to adjust the structure of causal forests such that the RR can be chosen as the quantity of interest. We present a novel method that uses generalized linear model (GLM) comparison as the basis for the forest splitting rule. Changing the link function of the GLM allows for different quantities to be targeted. This is implemented as an update to the **grf** software package in R (Tibshirani et al., 2023), with code available at <https://github.com/vshirvaikar/rref>.

The remainder of this report is organized as follows. In Section 2, we motivate the importance of relative risk. In Section 3, we present our proposed methodology and demonstrate how it fits into the causal forest framework. In Section 4, we validate our forest on simulated data, and in Section 5, we present real-world results on the LEADER clinical trial.

2 The importance of relative risk

Consider a clinical trial with n samples, each with covariates X_i , binary response $Y_i \in \{0, 1\}$, and binary treatment indicator $W_i \in \{0, 1\}$. Under the potential outcomes framework of Rubin (2005), define $Y_i^{(1)}$ and $Y_i^{(0)}$ as the i th subject’s potential response with and without the treatment respectively. Several different causal measures can be employed to report the treatment effect. Two of the most common choices are the (absolute) *Risk Difference* (RD)

$$\tau_{RD} = \mathbb{E} [Y_i^{(1)}] - \mathbb{E} [Y_i^{(0)}] \quad (1)$$

and the (relative) *Risk Ratio* (RR)

$$\tau_{RR} = \mathbb{E} [Y_i^{(1)}] / \mathbb{E} [Y_i^{(0)}] \quad (2)$$

where expected outcomes can be equivalently interpreted as probabilities since the outcome is binary

$$\mathbb{E} [Y_i^{(w)}] = \mathbb{P} [Y_i^{(w)} = 1] \quad (3)$$

Though we will not focus on them here, other measures used in the binary setting include the Odds Ratio (OR), which is often found in case-control studies; the Number Needed to Treat (NNT), which contextualizes the Risk Difference in terms of patient counts and frequently appears in medical practice; and the Survival Ratio (SR), which reverses the Risk Ratio to count null events (Cook and Sackett, 1995; Huitfeldt et al., 2022).

A frequent question of interest is treatment effect heterogeneity (TEH), or how the effect of the treatment varies across different subgroups of the study population (Rothman, 2012). Methods for TEH estimation, including causal forests, tend to focus on the *absolute* conditional average treatment effect (CATE)

$$\tau_{RD}(x) = E[Y_i^{(1)} - Y_i^{(0)} | X_i = x] \quad (4)$$

and maximize variance in this quantity, searching for subgroups where the treatment induces the largest absolute divergence in outcome. However, this may not be appropriate in a setting where baseline absolute risk levels vary widely as a function of initial covariates. For instance, Watson and Holmes (2020) present

a malaria case study from the AQUAMAT clinical trial (explored further in Section 4) where patients’ predicted risk of death at the start of treatment varied from less than 1% to greater than 80%. In this case, any estimates based on differences in absolute risk would be dominated by the covariates that predict overall mortality. Individuals with a high baseline risk at the beginning of treatment may be “over-represented” in the final results, since, for example, a reduction from 80% to 50% risk of $Y = 1$ would be considered roughly ten times as important as a reduction from 8% to 5%. This behavior is sensible in an overall analysis of the drug’s population-wide effect, but when looking specifically for TEH, it can dilute the method’s statistical power by discounting individuals with a low baseline risk level.

A more logical approach in this context might be to focus on differences in *relative* CATE

$$\tau_{RR}(x) = \frac{E[Y_i^{(1)} | X_i = x]}{E[Y_i^{(0)} | X_i = x]} \quad (5)$$

which would weight the 80% to 50% and 8% to 5% reductions equally. The relative Risk Ratio also presents other benefits related to explanation and generalizability, which we briefly outline as further motivation. Whether a treatment effect is reported in relative or absolute terms (for example, “five times larger” rather than “4% higher”) can significantly impact how its importance is interpreted. In practice, relative rates are often more intuitive to a doctor or patient, especially in cases where the outcome is rare (Altman, 1999).

RR has also been shown to extrapolate better across the medical literature, with relative risk reductions translating more effectively to different time periods or populations (Kuo et al., 2002; Spiegelman and VanderWeele, 2017). The question of “transportability” is closely related to TEH estimation, since both deal with how results from a (potentially unrepresentative) trial population can be generalized to an arbitrary target population. Colnet et al. (2023) show that the RR’s superior performance is related to its ability to disentangle treatment effect from baseline risk. This arises because the RR is both collapsible (meaning population effects can be written as a weighted average of subgroup effects, unlike the OR) and stable under population shifts (meaning no adjustment is needed for non-prognostic covariates, unlike the RD).

We therefore aim to provide a TEH estimation method which targets differences in relative risk. In the following section, we provide an overview of causal forests and generalized random forests, then demonstrate our proposed changes to the existing algorithm.

3 Modifying causal forests

Causal forests were developed by Athey and Imbens (2015) and Wager and Athey (2018) to enable the use of classical random forests (Breiman, 2001) for TEH discovery. In recent years, they have become extremely popular, applied to a variety of problems in the biomedical and social sciences (Davis and Heller, 2017; Athey and Wager, 2019; Raghavan et al., 2022).

3.1 Algorithm overview

A classical regression tree recursively partitions the input data into leaves L . The splitting algorithm is specified to maximize the difference across the split: for example, by minimizing the sum of the variances on each side. The observations in each leaf can then be considered alike, so we make a prediction for any new point x as the average of its leaf

$$\hat{\mu}(x) = \frac{\sum_{X_i \in L(x)} Y_i}{\#|X_i \in L(x)|} \quad (6)$$

For a causal tree, we analogously want each leaf to be small enough that it “acts as though [it] had come from a randomized experiment”, allowing us to draw conclusions about the average treatment effect for individuals within that specific subgroup (Wager and Athey, 2018). We assume unconfoundedness

$$\{(Y_i^{(0)}, Y_i^{(1)}) \perp\!\!\!\perp W_i\} | X_i \quad (7)$$

which means all the covariates that determine both potential outcomes and treatment assignment are included in X . The splitting algorithm is specified to target heterogeneity by maximizing the variation in $\hat{\tau}_{RD}(X_i)$. The (absolute) treatment effect for an individual is then the difference between the two treatment classes in its leaf

$$\hat{\tau}_{RD}(x) = \frac{\sum_{X_i \in L(x), W_i=1} Y_i}{\#|X_i \in L(x), W_i=1|} - \frac{\sum_{X_i \in L(x), W_i=0} Y_i}{\#|X_i \in L(x), W_i=0|} \quad (8)$$

Some additional changes must be made to the training and prediction procedure to ensure that results remain consistent and asymptotically normal under a causal framework. The key factor in this construction is a property known as honesty, which ensures that the splitting algorithm does not inappropriately incorporate information about the outcomes. This is achieved using a double-sample procedure:

1. Divide the training data into two halves I and J .
2. Use only the I sample to place regression splits.

3. Require that each leaf contains at least k observations of each treatment class in J .
4. Use only the J sample for within-leaf estimation and prediction.

This procedure is repeated for an ensemble of B trees, each based on a random subsample of $s < n$ training points. The split between I and J is re-randomized for each tree. The $\hat{\tau}_{RD}(x)$ predictions are then averaged across the B trees to yield final estimates. Computational implementations of causal forests often simplify this final step with a adaptive nearest-neighbor procedure: they look at how often all other points fall into the same leaf as the input x across the forest, then use those frequencies to compute a weighted average (Athey et al., 2019).

3.2 GLM-based node splitting

Any forest-based method is fundamentally defined by the rule that determines whether and where to split the data at a given node. Causal forests target absolute risk due to the optimization criterion used when splitting nodes – maximizing variation in $\hat{\tau}_{RD}(X_i)$. In order to target relative risk, we therefore need to modify this splitting procedure. We begin with a proposal for an alternative node-splitting procedure based on generalized linear models (GLM), then discuss how it can be specified to target relative risk.

Recall that our data at any given parent node consists of covariates X_i , response Y_i , and treatment indicator $W_i \in \{0, 1\}$. At any given node, for a candidate split value within X , we assign a binary variable $S_i \in \{0, 1\}$ that indicates whether an observation is on the left or right side of the split, as well as a treatment-split interaction term SW . We then run the GLM regression

$$Y \sim X + W + S + SW \quad (9)$$

The X terms regress out the baseline effect of the covariates, W accounts for the average treatment effect in the parent node, and S accounts for the average difference in outcomes across the split. SW then captures the strength of treatment effect heterogeneity induced by the split, and so we select the split candidate with the lowest p-value (most extreme test statistic) on the SW variable. This procedure is computationally intensive, but can be easily parallelized, and will generally be applied to long-term clinical trial analysis where runtime is not of primary concern¹.

¹Fitting a default 2,000-tree forest on a sample of size $n = 10,000$ with $d = 9$ dimensions (as seen in the simulation study in Section 4) takes about 20 minutes on a standard Dell Latitude personal laptop.

For high-dimensional cases, we use a pre-computed baseline risk Z in the regression rather than the full covariate matrix X , since the GLM model may fail to converge when the width of X exceeds the number of remaining data points at a given node. This could limit the power of our forest by preventing deeper trees with smaller leaves. We fit $Y \sim X\beta$ yielding coefficients $\hat{\beta}$ and set $Z = X\hat{\beta}$. Equation 9 then becomes

$$Y \sim Z + W + S + SW \quad (10)$$

Ultimately, the motivation for GLM-based splitting is that we can toggle our quantity of interest by changing the target distribution and link function of our GLM. Using linear regression, our procedure would target absolute risk, while with logistic regression, our procedure would target the odds ratio. To target relative risk, we use Poisson regression, which assumes the response has a Poisson distribution, and models the log of its expected value as a function of the covariates

$$Y_i \sim \text{Poisson}(\lambda_i) \\ \log(\lambda_i) = \beta_0 + \sum_{i=1}^j \beta_i x_i \quad (11)$$

Log-binomial regression (which instead assumes the response has a binomial distribution) is technically more accurate as it cannot return fitted probabilities greater than one, but Poisson regression uses a canonical link function, and the two methods have been shown to perform similarly in comparative studies (Petersen and Deddens, 2008; Chen et al., 2018).

The current state-of-the-art implementation of causal forests is the *causal_forest* function from the **grf** software package, written in R with back-end functions in C++ (Tibshirani et al., 2023). Generalized random forests (GRF) allow for the use of forest-based inference in a wide variety of statistical tasks, including TEH estimation (Athey et al., 2019). The GRF causal forest mirrors the previously outlined double-sample procedure, including honesty and subsampling, but with slight computational modifications for flexibility and performance. Our causal forest modifies the open-source **grf** code available on Github as described above; the code is available at <https://github.com/vshirvaikar/rref>. In the following two sections, we present results based on both simulated and real-world data.

4 Performance validation

To validate the relative risk (RR) causal forest, we test it against the original causal forest on simulated data with a known induced change in treatment effect heterogeneity (TEH).

4.1 Simulation procedure

The AQUAMAT study was an open-label, randomized clinical trial comparing artesunate and quinine for the treatment of severe falciparum malaria in African children (Dondorp et al., 2010; Leopold et al., 2019). The dataset consists of 5,425 samples with covariates X_i , binary response Y_i (where $Y = 1$ indicates death), and binary treatment indicator $W_i \in \{0, 1\}$ (randomized with a 50:50 allocation). Baseline pre-treatment risk (predicted as a function of covariates) ranged from roughly 0.03% to 84.2% with a mean of 9.7%, making this a good test case for relative risk methods.

Our aim was to develop a synthetic data generation procedure based on AQUAMAT that maintained a realistic covariance structure in X , while allowing the sample size and relative TEH level to be controlled. The temperature covariate served as the basis for induced cross-over heterogeneity; patients with an above-average temperature had their baseline risk increased, while patients with a below-average temperature had it decreased². The procedure was:

1. Fit a multivariate Gaussian model \mathcal{M} to the subset of nine continuous covariates. To allow a Gaussian \mathcal{M} , all binary covariates were dropped.
2. Generate n samples from \mathcal{M} .
3. Randomize treatment assignment $W \in \{0, 1\}$ with a 50:50 allocation.
4. Fit a binomial regression $Y \sim X$ using the original data and covariates, excluding temperature. Use the regression to predict each individual’s baseline risk level $\hat{p}_i = \mathbb{E}(Y_i|X_i)$.
5. For those who received treatment ($W = 1$), induce symmetric relative TEH. Multiply \hat{p}_i by a relative risk factor K if their temperature was above the median 38°C (yielding the updated $\hat{p}_i^* = K\hat{p}_i$), and divide it by K if it was below 38°C (yielding $\hat{p}_i^* = \hat{p}_i/K$).
6. Simulate individual $Y \in \{0, 1\}$ as Bernoulli(\hat{p}_i^*).
7. Train the original and relative risk forests with the default $B = 2,000$ trees and compare.

We repeated this procedure for 20 synthetic trials with $n = 10,000$ (approximating the size of the LEADER trial investigated in Section 5) and an 80:20 training-testing split. Each trial was run at relative risk levels $K \in \{1, 1.5, 2\}$ to explore how the forests’ relative performance changes as heterogeneity increases.

²Since our splitting rule is based on the interaction p-value, we would expect it to target cross-over or non-cross-over heterogeneity equally well.

4.2 Omnibus testing

Our main question of interest is whether the forests’ overall predictions of TEH are well-calibrated. The `grf` package includes a `test_calibration` function that assesses this based on a linear fit (Tibshirani et al., 2023). Specifically, let $\tilde{Y} = Y - \hat{Y}(X)$ and $\tilde{W} = W - \hat{W}(X)$ be the covariate-adjusted outcome and treatment vectors respectively. $\hat{\tau}(X_i)$ represents the causal forest’s predictions of heterogeneity, while $\bar{\tau}(X)$ indicates the causal forest’s mean prediction. The function fits the coefficients α and β in the linear equation

$$\tilde{Y} \sim \alpha \tilde{W} \bar{\tau}(X) + \beta \tilde{W} (\hat{\tau}(X_i) - \bar{\tau}(X)) \quad (12)$$

A coefficient near $\alpha = 1$ indicates that the mean forest prediction is centered, since a one-unit change in \tilde{W} approximately corresponds to a change of $\bar{\tau}(X)$ in \tilde{Y} , as expected. A coefficient of $\beta = 1$ indicates that the individual heterogeneity estimates from the forest are well-calibrated. Note that when $\alpha = \beta = 1$, Equation 12 reduces to $\tilde{Y} = \tilde{W} \hat{\tau}(X_i)$. The p-value on β is used as a significance test for overall evidence of heterogeneity in the data, since it means there is sufficient signal contained in the individual $\hat{\tau}(X_i)$ levels after adjusting for $\bar{\tau}(X)$.

We use a similar approach to modify this test for the relative Risk Ratio, again building upon Poisson regression in a GLM framework. Given a fitted causal forest, we can slightly modify Equation 8 to yield relative (rather than absolute) conditional average treatment effect estimates $\hat{\tau}_{RR}$ for each individual in the held-out test set. Starting with the baseline model $Y \sim X + W$, we then look at the ANOVA p-value of adding the additional term $\log(\hat{\tau}_{RR})$ to yield

$$Y \sim X + W + \log(\hat{\tau}_{RR}) \quad (13)$$

To calibrate the expected power of this test at $n = 10,000$, we generate several datasets using the procedure detailed above. We then replace $\log(\hat{\tau}_{RR})$ in Equation 13 with a binary indicator term T , which indicates whether each individual’s temperature is above or below 38, and therefore whether their baseline risk \hat{p}_i was adjusted up or down. This yields the equation

$$Y \sim X + W + T \quad (14)$$

where the p-value on T now represents the “true” ANOVA test p-value given the known correct model.

Figure 1 displays the fraction of 1,000 trials for which $p < 0.05$ on T as the induced heterogeneity K increases, which can be interpreted as the expected power of the test under the true model. This fraction first exceeds 80% at $K = 2$, which is the power level to which a sample size would typically be designed.

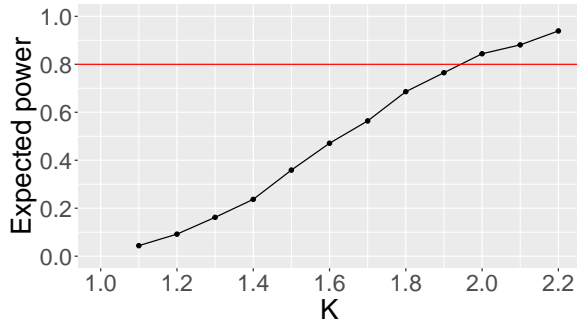


Figure 1: Fraction of 1,000 trials with $n = 10,000$ and induced relative TEH of K where ANOVA omnibus test on additional binary temperature indicator T returns $p < 0.05$. Under the specified procedure, expected power first exceeds 80% (red) at $K = 2$.

K	Forest Median		RR wins out of 20
	Original	RR	
1	0.550	0.576	10
1.5	0.533	0.456	13
2	0.010	0.006	15

Table 1: Median ANOVA omnibus test p-values on additional $\log(\hat{\tau}_{RR})$ term as induced heterogeneity K increases, and number of trials (out of 20) where RR forest has a lower p-value.

We therefore should expect the difference between the original and RR forests to become clear at this level³. Any loss in power from the curve in Figure 1 to the causal forests is a result of the forest design, which requires searching through covariates that are known not to affect heterogeneity under the simulation protocol.

Figure 2 compares the $-\log_{10}(\text{p-values})$ across the 20 causal forest trials, with summary metrics in Table 1. As K increases, both forests return lower p-values, and therefore higher $-\log_{10}(\text{p-values})$. The forests’ performance is comparable for $K = 1.5$, but as expected, the RR forest’s predictions appear better-calibrated at $K = 2$, with the large majority of points falling below the 45-degree line. Overall, these results suggest that the RR forest can provide clear benefits in identifying relative heterogeneity, and that its performance improves as the level of heterogeneity increases.

³We note that $K = 2$ is a larger treatment effect than would realistically be expected in a new drug trial. However, the original AQUAMAT trial was powered at 80% for a 25% reduction in mortality and used $n = 5,000$; under the rule of thumb that interactions need four times the sample size as a main effect, it approximately aligns that we need twice the sample size for an interaction effect which is twice as large.

K	Forest Median		RR wins out of 20
	Original	RR	
1	7.4%	5.5%	7
1.5	41.0%	47.8%	14
2	62.1%	63.4%	17

Table 2: Median variable importance assigned to temperature as induced heterogeneity K increases, and number of trials (out of 20) where RR forest successfully identifies temperature as more important.

4.3 Variable importance

If the relative risk causal forest is outperforming the original causal forest, it should also identify temperature as the relevant splitting covariate more often and at a lower depth (further up the tree). The `grf` software package provides a built-in *variable importance* summary metric that calculates this for a given forest (Tibshirani et al., 2023).

Figure 3 compares the variable importance assigned to temperature across the 20 trials. Graphically, we observe that as the heterogeneity level K increases, both forests assign more importance to temperature, but more of the points fall below the black 45-degree line, indicating that the RR forest becomes relatively better at identifying temperature as the critical covariate. These results are summarized in Table 2.

5 Application: LEADER trial

The Liraglutide Effect and Action in Diabetes: Evaluation of Cardiovascular Outcome Results (LEADER) trial was initiated in 2010 to evaluate the benefit of liraglutide, a glucagon-like peptide 1 analogue, in the treatment of patients with type 2 diabetes (Marso et al.). 9340 patients underwent randomization with a median follow-up time of 3.8 years; the primary outcome (MACE, or major adverse cardiovascular events) occurred in significantly fewer patients in the treatment group⁴. In this section, we compare results from the baseline and GLM forests, and discuss the strength of evidence for overall heterogeneity in LEADER.

5.1 Data setup

From the LEADER dataset, 70 covariates were identified as potentially relevant based on guidance from collaborators at Novo Nordisk, including a mix of demographic fields, vital signs, lab measurements, medical history flags, and medication flags. Details can be

⁴13.0% compared to 14.9%, with a hazard ratio of 0.87 (95% confidence interval from 0.78 to 0.97)

found in the supplementary material. The predicted baseline risk of MACE as a function of the selected covariates ranged from 1.2% to 62.4% with a mean of 13.9%. We used only the 8,750 out of 9,340 patients who had no missing data across these covariates; this subset had a very similar outcome distribution to the complete data. The original and RR causal forest algorithms were each trained on 80% of this data with the remaining 20% held out for omnibus testing. The number of trees for each forest was increased to $B = 5,000$ ⁵.

5.2 Omnibus testing

With the built-in *test_calibration* function, the original causal forest returns a p-value of 0.825 on the β coefficient, suggesting a lack of overall (absolute) heterogeneity in the data.

Using the ANOVA test introduced in Section 4.2, the original forest returns a p-value of 0.390 while the RR forest returns a p-value of 0.856, also indicating that neither forest was able to find significant evidence of heterogeneity.

5.3 Variable importance

To compare the original and RR forests, we also look at differences in which variables were identified as important. Table 3 shows the top six variables which gain the most weight in the RR forest. These are covariates which may be overlooked in an absolute risk setting, but which relative risk reveals to be potentially important sources of heterogeneity. The RR forest can therefore serve as a discovery tool for further qualitative analysis of TEH. In this case, whereas the original forest assigns slightly higher weights to medical history and medication flags, the RR forest shifts much of this weight towards baseline demographic and lab measurements.

Specific investigation of the top variables in Table 3 reveals interesting trends, though as with all post-hoc analysis, these results should be interpreted with caution. For instance, Figure 4 displays the relative treatment effect for DIABDUR (diabetes duration in years), the most important variable in the RR forest, broken down by quintile and adjusted for all other covariates. Based on the 95% standard errors, we observe that the relative treatment effect is most significant for the lowest quintile (individuals who have had diabetes for up to 6 years.)

⁵In simulation, we found 5,000 trees to be a stable forest size after which the average importance assigned to any individual variable would fluctuate by no more than 0.1%.

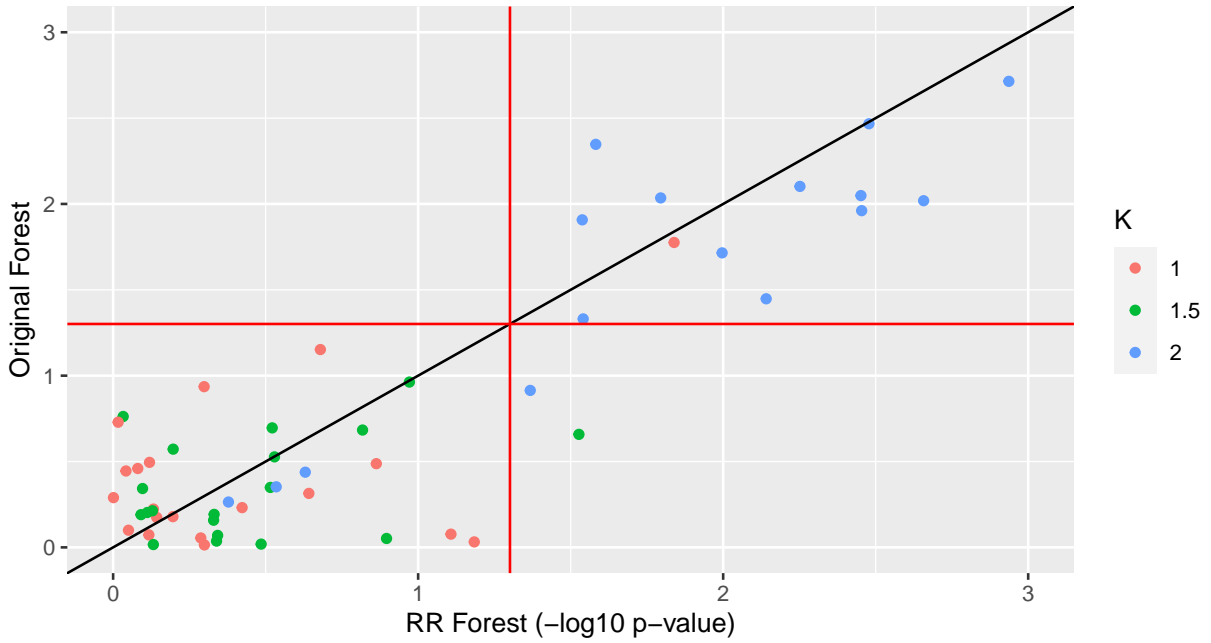


Figure 2: ANOVA omnibus test $-\log_{10}(\text{p-values})$ on additional $\log(\hat{\tau}_{RR})$ term for each of 20 causal forest trials with $n = 10,000$ and induced relative TEH of K . Red lines indicate significance cutoff at $-\log_{10}(0.05) = 1.3$. Points below the 45-degree line indicate that the RR forest had a lower p-value than the baseline forest, which we would expect in cases where $K > 1$.

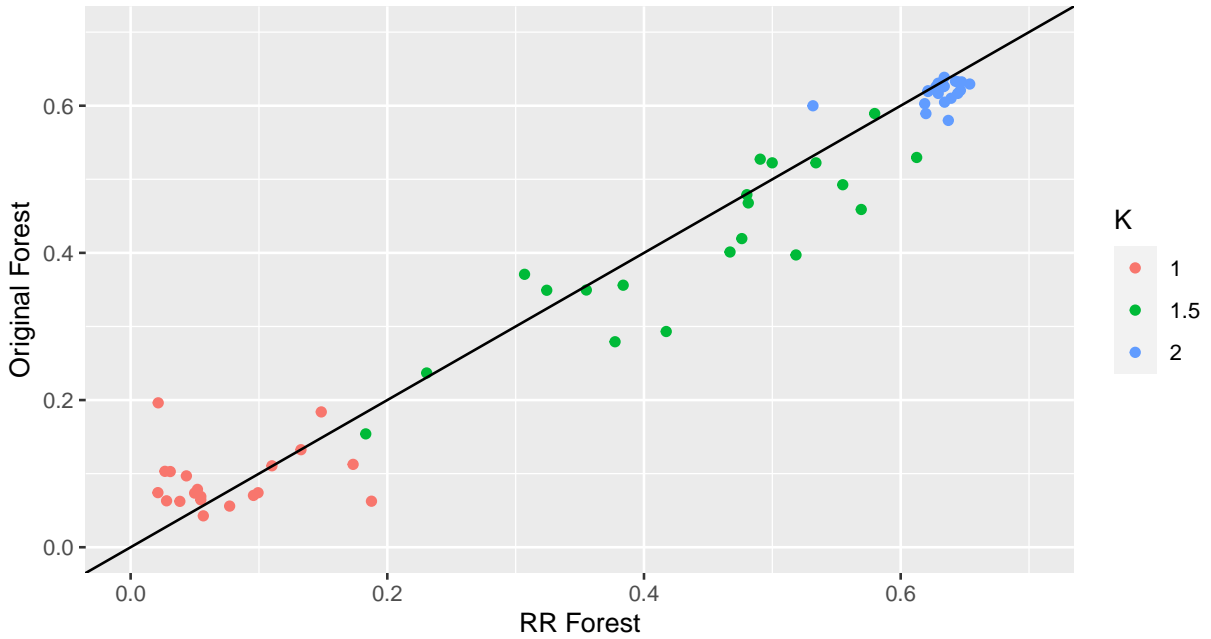


Figure 3: Variable importance assigned to temperature for each of 20 causal forest trials with $n = 10,000$ and induced relative TEH of K . Points below the 45-degree line indicate that the RR forest found temperature to be more important than the baseline forest, which we would expect in cases where $K > 1$.

Variable	Forest Importance	
	Original	RR
DIABDUR	5.3%	13.9%
LDL1BL	4.8%	9.7%
AGE	4.6%	9.3%
CREATBL	2.7%	5.9%
WSTCIRBL	3.4%	6.6%
SYSBPBL	2.4%	4.9%

Table 3: Variables with the largest increase in importance between original and RR causal forests. DIA-BDUR is diabetes duration; AGE is age; LDL1BL, CREATBL, WSTCIRBL, and SYSBPBL are baseline “bad” cholesterol, creatine, waist circumference, and systolic blood pressure respectively.

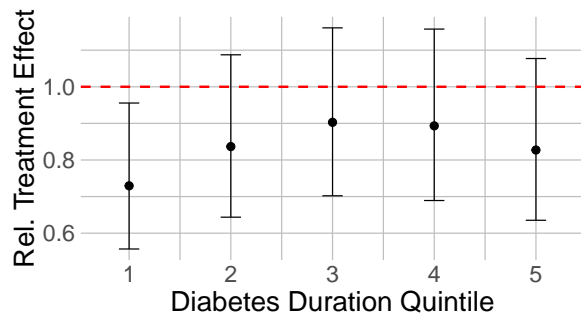


Figure 4: Covariate-adjusted relative treatment effect with 95% standard errors by quintile for DIABDUR (diabetes duration in years), the most important variable in the RR forest.

6 Conclusion

In this study, we present relative risk forests as an adaptation of causal forests that specifically targets heterogeneity in the relative Risk Ratio (RR). The RR is an important clinical measure due to its ability to generalize across populations; TEH discovery methods that only target the absolute Risk Difference (RD) may therefore overlook critical sources of heterogeneity on the RR scale, especially in settings with large variation in individual baseline risk.

The modification is based on an alternative splitting rule for the data in a causal forest that uses generalized linear model (GLM) comparison. Specifying Poisson regression as the GLM of choice allows the RR to be targeted as the quantity of interest. We validate the forests’ performance on simulated data, using variable importance and an ANOVA-based omnibus test for evaluation, and present real-world results and discussion from the LEADER clinical trial.

Acknowledgements

We thank James Watson, Kate Ross, George Nicholson, and Edwin Fong for their helpful feedback. We also thank collaborators at Novo Nordisk for their guidance and suggestions. VS is supported by the EPSRC Centre for Doctoral Training in Modern Statistics and Statistical Machine Learning (EP/S023151/1) and Novo Nordisk. CH is supported by the EPSRC Bayes4Health programme grant and The Alan Turing Institute, UK.

References

- D. G. Altman. *Practical statistics for medical research*. Chapman & Hall, Boca Raton, Fla, 1999. ISBN 9780412276309.
- S. Athey and G. Imbens. Recursive Partitioning for Heterogeneous Causal Effects. *arXiv:1504.01132*, Dec. 2015.
- S. Athey and S. Wager. Estimating treatment effects with causal forests: An application. 2019.
- S. Athey, J. Tibshirani, and S. Wager. Generalized random forests. *The Annals of Statistics*, 47(2): 1148–1178, Apr. 2019. ISSN 0090-5364, 2168-8966.
- S. Basu, S. Raghavan, D. J. Wexler, and S. A. Berkowitz. Characteristics Associated With Decreased or Increased Mortality Risk From Glycemic Therapy Among Patients With Type 2 Diabetes and High Cardiovascular Risk: Machine Learning Analysis of the ACCORD Trial. *Diabetes Care*, 41(3): 604–612, Mar. 2018. ISSN 0149-5992, 1935-5548.
- L. Breiman. Random forests. *Machine Learning*, 45 (1):5–32, 2001. ISSN 08856125.
- W. Chen, L. Qian, J. Shi, and M. Franklin. Comparing performance between log-binomial and robust Poisson regression models for estimating risk ratios under model misspecification. *BMC Medical Research Methodology*, 18(1):63, June 2018. ISSN 1471-2288.
- B. Colnet, J. Josse, G. Varoquaux, and E. Scornet. Risk ratio, odds ratio, risk difference... which causal measure is easier to generalize? *arXiv:2303.16008*, 2023.
- D. I. Cook, V. J. Gebski, and A. C. Keech. Subgroup analysis in clinical trials. *Medical Journal of Australia*, 180(6):289–291, Mar. 2004. ISSN 0025-729X, 1326-5377.
- R. J. Cook and D. L. Sackett. The number needed to treat: a clinically useful measure of treatment effect. *310(6977):452–454*, 1995. ISSN 0959-8138, 1468-5833.
- J. M. Davis and S. B. Heller. Using Causal Forests to Predict Treatment Heterogeneity: An Application

- to Summer Jobs. *The American Economic Review*, 107(5):546–550, 2017. ISSN 0002-8282.
- A. M. Dondorp, C. I. Fanello, I. C. Hendriksen, E. Gomes, A. Seni, K. D. Chhaganlal, K. Bojang, R. Olaosebikan, N. Anunobi, K. Maitland, E. Kivaya, T. Agbenyega, S. B. Nguah, J. Evans, S. Gesase, C. Kahabuka, G. Mtove, B. Nadjm, J. Deen, J. Mwanga-Amumpaire, M. Nansumba, C. Karema, N. Umulisa, A. Uwimana, O. A. Mokuolu, O. T. Adedoyin, W. B. Johnson, A. K. Tshefu, M. A. Onyamboko, T. Sakulthaew, W. P. Ngum, K. Silamut, K. Stepniewska, C. J. Woodrow, D. Bethell, B. Wills, M. Oneko, T. E. Peto, L. Von Seidlein, N. P. Day, and N. J. White. Artesunate versus quinine in the treatment of severe falciparum malaria in African children (AQUAMAT): an open-label, randomised trial. *The Lancet*, 376(9753):1647–1657, Nov. 2010. ISSN 01406736.
- A. Huitfeldt, M. P. Fox, E. J. Murray, A. Hróbjartsson, and R. M. Daniel. Shall we count the living or the dead? *arXiv:2106.06316*, 2022.
- J. Kuo, I. Linkov, L. Rhomberg, M. Polkanov, G. Gray, and R. Wilson. Absolute Risk or Relative Risk? A Study of Intraspecies and Interspecies Extrapolation of Chemical-Induced Cancer Risk. *Risk Analysis*, 22(1):141–157, Feb. 2002. ISSN 02724332, 15396924.
- S. J. Leopold, J. A. Watson, A. Jeeyapant, J. A. Simpson, N. H. Phu, T. T. Hien, N. P. J. Day, A. M. Dondorp, and N. J. White. Investigating causal pathways in severe falciparum malaria: A pooled retrospective analysis of clinical studies. *PLoS Medicine*, 16(8):e1002858, Aug. 2019. ISSN 1549-1676.
- S. P. Marso, G. H. Daniels, K. Brown-Frandsen, P. Kristensen, J. F. Mann, M. A. Nauck, S. E. Nissen, S. Pocock, N. R. Poulter, L. S. Ravn, W. M. Steinberg, M. Stockner, B. Zinman, R. M. Bergental, and J. B. Buse. Liraglutide and cardiovascular outcomes in type 2 diabetes. 375(4):311–322. ISSN 0028-4793, 1533-4406.
- M. R. Petersen and J. A. Deddens. A comparison of two methods for estimating prevalence ratios. *BMC Medical Research Methodology*, 8(1):9, Feb. 2008. ISSN 1471-2288.
- S. Raghavan, K. Josey, and D. Ghosh. Generalizability of heterogeneous treatment effects based on causal forests applied to two randomized clinical trials of intensive glycemic control. *Annals of Epidemiology*, Jan. 2022.
- K. J. Rothman. *Epidemiology: an introduction*. Oxford Univ. Press, New York, NY, 2nd edition, 2012. ISBN 9780199754557.
- D. B. Rubin. Causal Inference Using Potential Outcomes: Design, Modeling, Decisions. *Journal of the American Statistical Association*, 100(469):322–331, Mar. 2005. ISSN 0162-1459, 1537-274X.
- D. Spiegelman and T. J. VanderWeele. Evaluating Public Health Interventions: 6. Modeling Ratios or Differences? Let the Data Tell Us. *American Journal of Public Health*, 107(7):1087–1091, July 2017. ISSN 0090-0036, 1541-0048.
- J. Tibshirani, S. Athey, E. Sverdrup, and S. Wager. *grf: Generalized Random Forests*, 2023. URL <https://github.com/grf-labs/grf>. R package version 2.3.0.
- S. Wager and S. Athey. Estimation and inference of heterogeneous treatment effects using random forests. *Journal of the American Statistical Association*, 113(523):1228–1242, July 2018. ISSN 0162-1459.
- J. A. Watson and C. C. Holmes. Graphing and reporting heterogeneous treatment effects through reference classes. *Trials*, 21(1):386, May 2020. ISSN 1745-6215.

Supplementary Material: Targeting Relative Risk Heterogeneity with Causal Forests

A List of variables included in LEADER analysis

- **6 demographic fields:** AGE (Age), DIABDUR (Diabetes Duration), SEX (Sex), RACE (Race), SMOKER_CURR (Current Smoker), SMOKER_PREV (Previous Smoker)
- **11 baseline vital signs:** WSTCIRBL (Waist Circumference at Baseline), BMIBL (Body Mass Index at Baseline), PULSEBL (Pulse at Baseline), SYSBPBL (Systolic BP at Baseline), DIABPBL (Diastolic BP at Baseline), HBA1CBL (HbA1c at Baseline), HDL1BL (HDL Cholesterol at Baseline), LDL1BL (Calc. LDL Cholesterol at Baseline), CHOL1BL (Total Cholesterol at Baseline), TRIG1BL (Triglycerides at Baseline), CREATBL (Serum Creatinine at Baseline)
- **14 lab measurements:** ALT (Alanine Aminotransferase), AMYLASE (Amylase), BILI (Bilirubin), CA (Calcium), EGFRCKD (EGFR using CKD-EPI Method), EGFRMDRD (EGFR using MDRD Method), K (Potassium), LIPASE (Triacylglycerol Lipase), SODIUM (Sodium), HCT (Hematocrit), HGB (Hemoglobin), PLAT (Platelets), RBC (Erythrocytes), WBC (Leukocytes)
- **19 medical history flags:** AHYPERFL (Antihypertensive Therapy Flag), MIFL (Myocardial Infarction Flag), STROKEFL (Stroke Flag), STROKSFL (Stroke Flag Sensitivity Analysis), REVASFL (Revascularization Flag), STENFL (Carotid Stenosis on Angiography Flag), CHDFL (Coronary Heart Disease Flag), IHDFL (Ischaemic Heart Disease Flag), CHFFL (Chronic Heart Failure NYHA II-III Flag), KIDFL (Chronic Kidney Failure Flag), MICFL (Microalbuminuria or Proteinuria Flag), HYPFL (Hypertension and LVH Flag), LVSDFL (Left Ventricular Systolic and Diastolic Dysfunction Flag), PADFL (Ankle/Brachial Index Flag), CVHIFL (CV High Risk Group Flag), CVMEDFL (CV Medium Risk Group Flag), RETSCRFL (Diabetic Retinopathy at Screening Flag), NEPSCRFL (Diabetic Nephropathy at Screening Flag)
- **20 concomitant medication flags:** CM_A10A (Insulin), CM_A10B_AD (Metformin), CM_A10BB (SU), CM_A10BF (Alpha glucosinade inhibitors), CM_A10BG (TZD), CM_A10BX (Glinides), CM_B01AA (Vitamin K antagonists), CM_B01AC (Platelet inhibitors), CM_C02 (Other antihypertensives), CM_C03A (Thiazides), CM_C03BA (Thiazide-like diuretics), CM_C03C (Loop diuretics), CM_C03DA (Aldosterone antagonists), CM_C07 (Beta-blockers), CM_C08 (Calcium channel blockers), CM_C09_AB (ACE inhibitors), CM_C09_CD (Angiotensin receptor blockers), CM_C10AA (Statins), CM_C10A_BCD (Other lipid lowering drugs), CM_C10AX (Ezetimibe)